

Optical response and emission waveguiding in rubrene crystalsS. Tavazzi,¹ A. Borghesi,¹ A. Papagni,¹ P. Spearman,^{1,2} L. Silvestri,^{1,3} A. Yassar,⁴ A. Camposeo,⁵ M. Polo,⁵ and D. Pisignano⁵¹*Dipartimento Scienza dei Materiali, Università di Milano Bicocca, Via Cozzi 53, I-20125 Milano, Italy*²*School of Chemical and Pharmaceutical Sciences, Kingston University, Kingston upon Thames, KT1 2EE, United Kingdom*³*Scuola Normale Superiore, Piazza dei Cavalieri 7, I-56100 Pisa, Italy*⁴*ITODYS, Université Paris7-Denis Diderot, 1, rue Guy de la Brosse, 75005 Paris, France*⁵*National Nanotechnology Laboratory of CNR-INFN, Distretto Tecnologico ISUFI, Università di Lecce, via Arnesano, I-73100 Lecce, Italy*

(Received 26 April 2007; published 14 June 2007)

The optical response of rubrene crystals is described by providing the full UV-VIS dielectric tensor. Consistently with the molecular and crystal symmetries, the lowest crystal transition originates from an A_u molecular transition, it is polarized along the c axis (normal to the larger crystal face), and it is the origin of the emission, which is self-guided towards the edge where the corresponding polarization and intensity angular distribution are detected. By contrast, the B_u molecular transitions give rise to Davydov states described by the other two components of the diagonal dielectric tensor.

DOI: [10.1103/PhysRevB.75.245416](https://doi.org/10.1103/PhysRevB.75.245416)

PACS number(s): 78.55.Kz, 78.40.-q, 71.35.Cc, 78.20.Ci

I. INTRODUCTION

Among the different organic materials, rubrene, a derivative of tetracene with phenyl substituents, has recently been gaining much attention due to its optoelectronic properties.¹⁻⁵ While its high carrier mobility is well documented, there are relatively few studies on the optical properties of crystalline rubrene, which are fundamental for developing new strategies in device design. To date, ellipsometry measurements have been reported⁶ and the isotropic dielectric function deduced only in the case of polycrystalline rubrene films deposited by evaporation on silicon substrates. In the single crystal form, its strong anisotropy has prevented a full optical characterization, thus limiting the understanding of the intermolecular interactions in the solid.

In this paper, the full UV-VIS dielectric tensor of rubrene crystals is provided and rationalized. Two components along the a and b crystallographic axes give information on intermolecular interactions and Davydov splitting of the B_u molecular transitions. By contrast, the lowest crystal transition originates from the lowest A_u molecular excited state and its dipole moment lies along the c axis, normal to the most developed crystal face. Photoluminescence originating from this transition is demonstrated to be self-guided towards the edge where the polarization and angular distribution are measured.

II. EXPERIMENT

Rubrene powder was purchased from Acros Organics and crystals with base centered orthorhombic structure⁷⁻⁹ were grown by physical vapor transport with thicknesses of the order of several μm . The crystal space group is D_{2h}^{18} and its factor group is D_{2h} . The unit cell with axes $a=7.2 \text{ \AA}$, $b=14.4 \text{ \AA}$, $c=26.9 \text{ \AA}$ (we adopt this notation from Refs. 4 and 8 although different notations are found in the literature) contains four molecules and is 2 times the primitive cell.

Images of the crystals were taken under a Leica PL inverted microscope fitted with a monochrome camera Axio-

Cam MR (Zeiss) microscope. Absorbance spectra were taken at room temperature using a Perkin-Elmer Lambda 900 spectrometer equipped with Glan-Taylor calcite polarizers. Reflectance and variable-angle ellipsometry measurements were performed using a VASE ellipsometer from J.A. Woollam Co. Inc. Polarized and angle-resolved photoluminescence (PL) spectra were taken by fixing a multimode optical fiber on a rotating stage, 2 cm away from the crystal surface and using a monochromator, a CCD detector, and a polarization filter to analyze the PL polarization state. The samples were excited at normal incidence with a 3.0 eV semiconductor diode laser (the spot size is 1 mm^2 , the crystal area was few tens of mm^2 , the distance of the excitation spot from the edge was smaller than 1 mm).

III. RESULTS AND DISCUSSION

Rubrene molecules in the crystal present C_{2h} symmetry with the twofold axis of rotation along the short backbone axis M . The molecular dipole-allowed excited states have symmetry either A_u or B_u with dipole moments along M and in the LN plane, respectively, where L is the long molecular axis and N the normal to the backbone plane [Fig. 1(a)]. In the crystal, the L axes lie in the ab plane (the most developed face), the short axes M lie along c . Optical transitions in the molecule were calculated using HyperChem (version 7.52, Hypercube Inc.) with ZINDO/S which uses theoretically based intermediate neglect of differential overlap (INDO) parametrized to reproduce spectroscopic transitions with a configuration interaction (CI) including all singly excited configurations with 10 eV limit between the occupied and unoccupied orbitals. The starting molecular geometry was extracted from Ref. 8 followed by geometry optimization performed using the restricted Hartree-Fock Austin model 1 (AM1) method. Since the same molecular geometry was assumed for both ground and excited states, the calculated energies can be overestimated, but the order and polarization of the transitions are provided, which are of special interest for the comprehension of the crystal spectra. The calculated

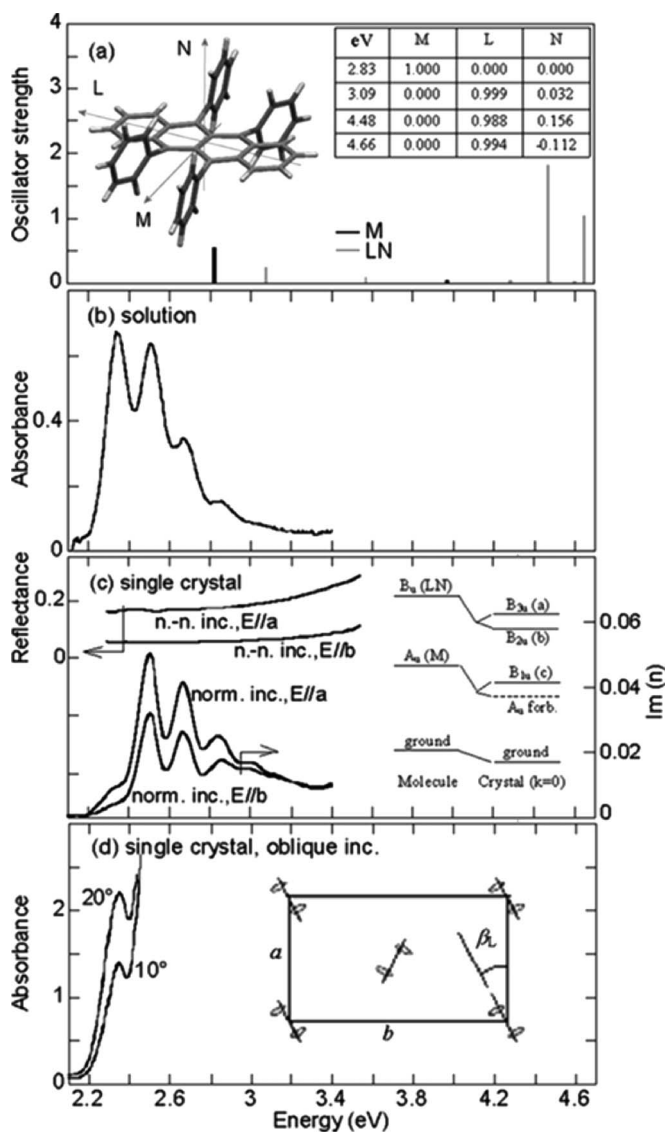


FIG. 1. (a) Oscillator strength of the calculated electronic transitions of the rubrene molecule. Inset: sketch of the molecule showing the direction of the M , L , and N axes. Table: direction cosines along M , L , and N axes of the four most relevant transitions. (b) Absorbance spectrum of rubrene in chloroform solution. (c) Near-normal incidence reflectance spectra of a rubrene single crystal taken with either a or b polarized light and the imaginary part of the refractive index deduced from the normal-incidence absorbance spectra of a $5 \mu\text{m}$ rubrene single crystal taken with a and b polarized light. Inset: scheme of the electronic energy levels from the isolated molecule to the single crystal. (d) Absorbance spectra of a rubrene single crystal at 10° and 20° angles of incidence with bc as plane of incidence and p (bc) polarized light. Inset: view of the arrangement of the molecules in the ab plane and of the β_L angle between the a axis and the molecular backbone.

strongest transitions [Fig. 1(a) and the table in the inset] are at 2.83 eV (M polarized) and at 3.09, 4.48, and 4.66 eV (LN polarized). In the crystal, the ab plane coincides with the molecular mirror plane, so that the site group is again C_{2h} . The excited states at the center of the Brillouin zone can be classified according to the irreducible representations of the factor group D_{2h} . Dipole-allowed crystal excited states have

B_{1u} , B_{2u} , or B_{3u} symmetry with transition dipole along c , b , and a , respectively. Each A_u excited state gives rise to a dipole-allowed transition with c polarization (B_{1u} symmetry), while B_u transitions give Davydov components polarized along a (B_{3u}) and b (B_{2u}).¹⁰

Figure 1(b) shows the spectrum of rubrene in chloroform solution with the same bands as reported in the literature.^{11–15} The lowest peak in solution is measured at 2.35 eV, red-shifted with respect to the calculated energy in vacuum (2.83 eV). This difference is attributed partially to the effects of the environment (the solvent) and to the fact that the calculated energy for the isolated molecule is overestimated. A further absorption band of rubrene in solution is reported at about 4.1 eV in Ref. 15, corresponding to the calculated one at 4.48 eV.

Figure 1(c) shows the reflectivity curves of a rubrene single crystal taken at near-normal incidence for either a or b polarized incident light, together with the imaginary parts of the refractive indexes deduced by correcting the transmittance T_m measured at normal incidence by the reflectivity contribution R [$T = T_m / (1 - R)$] and multiplying the corresponding absorbance (absorbance = $-\log T$) by $\lambda \ln 10 / (4\pi d)$, where λ is the wavelength of light and d is the sample thickness. Above 3.6 eV, the spectrum is omitted due to absorbance saturation. Both the a and b polarized spectra of the single crystal taken at normal incidence show vibronic progressions with main peaks at 2.50 eV, 2.67 eV, 2.86 eV. A weak shoulder is also detected centered at about 2.32 eV. We attribute these progressions to a and b polarized excitonic transitions originating from the molecular transition at 3.09 eV with LN polarization [see inset of Fig. 1(c)]. Similarly, Mitrofanov *et al.*¹⁶ detected a vibronic series with a weak absorption band at 2.32 eV and attributed it to the 0-0 transition of the progression. We underline the weak intensity of this 0-0 band. As seen in the inset of Fig. 1(d), the molecular L axes lie in the ab plane at an angle $\beta_L = 31^\circ$ (Refs. 7–9) with respect to the a axis. The transition moments of the LN polarized molecular transitions are also symmetrically oriented at an angle β with the a axis. From β_L and the values shown in the inset table of Fig. 1(a), β is found 33° for the transition at 3.09 eV. The polarization of the crystal states is given by the sum and difference of the two non-equivalent molecular transition moments.¹⁰ It follows that allowed transitions in the crystal of LN origin are either a or b polarized with intensity ratio $\cotan^2 \beta$. This ratio is measured to be about 1.7, so that β is 37° , in satisfactory agreement with the predicted value of 33° . It can be seen that the a and b structures are superimposed, i.e., the Davydov splitting is negligible, thus indicating weak intermolecular interaction and weak exciton delocalization.¹⁰ Figure 1(d) shows a portion of the absorbance spectra of a rubrene crystal at oblique incidence with bc as plane of incidence and p (bc) polarized light. An emerging peak at about 2.35 eV is detected. This peak does not coincide with any band in the spectra of the single crystal taken at normal incidence. It is at about the same energy as the lowest absorption peak of the molecule in solution, and is attributed to the c polarized transition in the crystal of M molecular origin in the presence of weak intermolecular interactions.¹⁰ We underline that the

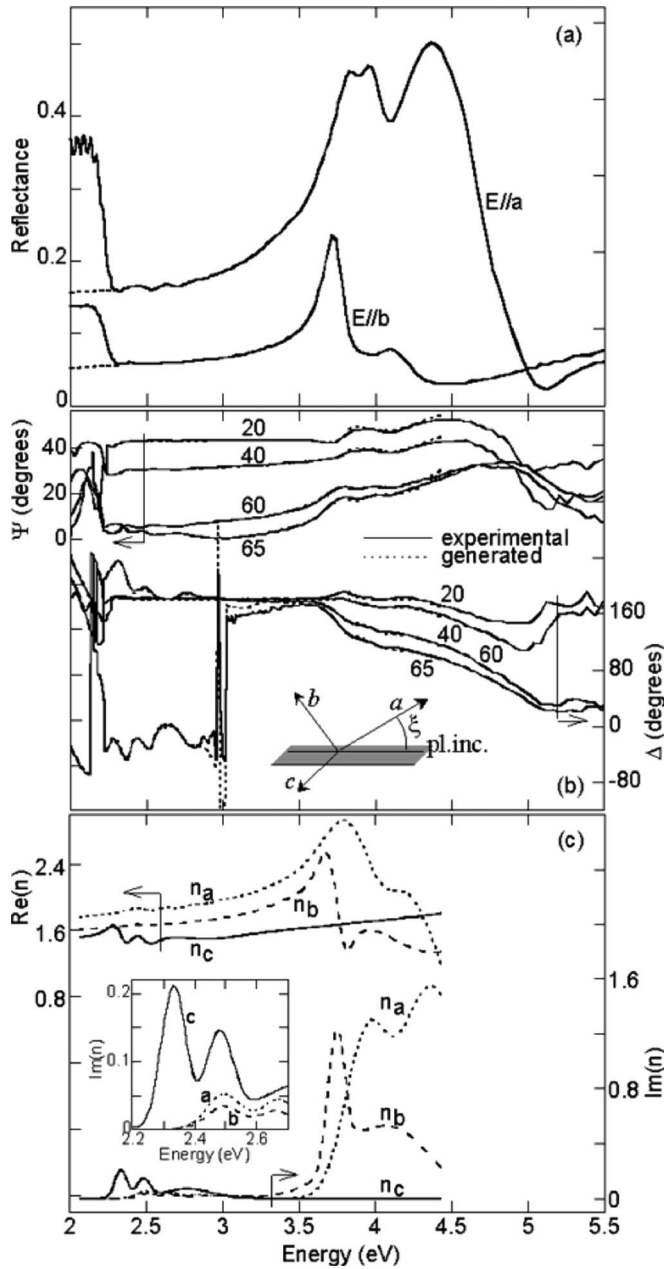


FIG. 2. (a) Near-normal incidence reflectance of a rubrene single crystal taken with a and b polarized light. The extrapolated reflectivity below 2.2 eV is shown with dotted lines. (b) Ellipsometry angles ψ and Δ as measured (continuous lines) or generated by the fitting of the measured data (dotted lines) at different angles of incidence from 20° to 65° on the ab face of a rubrene single crystal using a plane of incidence which forms an angle $\xi=33^\circ$ to the ac rubrene plane. Inset: sketch of the experimental configuration. (c) Real and imaginary parts of the refractive indexes \hat{n}_a , \hat{n}_b , and \hat{n}_c of rubrene single crystals obtained by the fitting of the ellipsometry data. Inset: imaginary parts on an enlarged scale.

lowest M polarized molecular transition gives rise to transitions which are superimposed in solution and in the crystal. The crystal transition can be discriminate with appropriate polarization at oblique incidence.

To deduce the full dielectric tensor, reflectance [Fig. 2(a)] and ellipsometry [Fig. 2(b)] measurements were performed.

Besides weak structures at low energy, the near-normal incidence reflectance spectra are dominated by a few bands above 3.6 eV, while the increase in intensity below 2.2 eV is due to the light reflected from the back sample surface. These curves were used to determine, in first approximation, the a and b optical functions using the Kramers-Kronig (KK) relations¹⁷ by extrapolating the reflectivity at low energy by the dashed lines in Fig. 2(a) and above $E_{\max}=5.5$ eV by $R(E)=R(E_{\max})\frac{E_{\max}^p}{E^p}$, with p adjusted such that $\text{Im}(\hat{n})$ deduced by the KK relations agrees with the values below 3.6 eV in Fig. 1(c).¹⁸ Ellipsometry measurements were performed rotating the crystal around the c axis [the plane of incidence forming an angle ξ with the rubrene ac plane, inset of Fig. 2(b)]. The ratios between the elements of the Jones matrix¹⁹ $\hat{r}_{pp}/\hat{r}_{ss}=\tan(\psi)e^{i\Delta}$ [Fig. 2(b), continuous lines], $\hat{r}_{ps}/\hat{r}_{pp}$, and $\hat{r}_{sp}/\hat{r}_{ss}$ were acquired. For simplicity, we considered the region below 4.4 eV. The data were analyzed with the program WVASE 32 based on generalized ellipsometry.²⁰ The sample is modeled as a biaxial bulk material with parametrized dielectric functions along a , b , and c given by Lorentz oscillators.^{17,21} The energies of the a and b transitions below 3 eV were assumed fixed consistently with the crystal spectra in Fig. 1(c). In addition, the optical functions deduced by the KK relations were used to determine the starting values of the other a and b free parameters before the fitting procedure. The results of the fitting and the obtained optical functions are shown in Figs. 2(b) and 2(c), respectively (ξ was found at 33°, in agreement with the sample orientation during the measurement). For the a and b polarizations, besides the progressions at low energy, the intense transitions at about 4 eV and at 3.75 eV, respectively, are attributed to excitonic transitions separated by a Davydov splitting originating from the B_u molecular transition at 4.48 eV. By contrast, the c component shows a progression originating from the lowest M molecular transition, whose first peak was probed in Fig. 1(d). The isotropic optical functions reported in Ref. 6 as deduced by ellipsometry measurements on rubrene films show intermediate values with respect to the components of the full dielectric tensor here reported, as expected. In particular, the lowest peak in the imaginary part of the optical function reported by Xie *et al.*⁶ corresponds to the c polarized band at 2.35 eV with similar absolute values, while at higher energy the different optical responses along the different crystallographic directions are mixed. We emphasize that, in a recent paper, Käfer *et al.*²² showed that rubrene crystals can be naturally oxidized with a depth profile for the rubrene peroxide concentration. The relative concentration is found to be about 1% at a depth of 50 nm and of the order of 0.1% at a depth of 150 nm. On the basis of these findings, we have checked the changes in the ellipsometry curves after adding a layer on top of the biaxial rubrene crystal with thickness of 150 nm and optical properties described by an effective-medium-approximation (EMA) assuming indicative values for the rubrene bulk component (98%) and for void (2%). EMA layers including an artificial fraction of void are typically used to simulate small variations of the refractive index.²³ No significant differences are observed in the ellipsometry data with or without the EMA layer, the only effect being a slight variation in the fitting

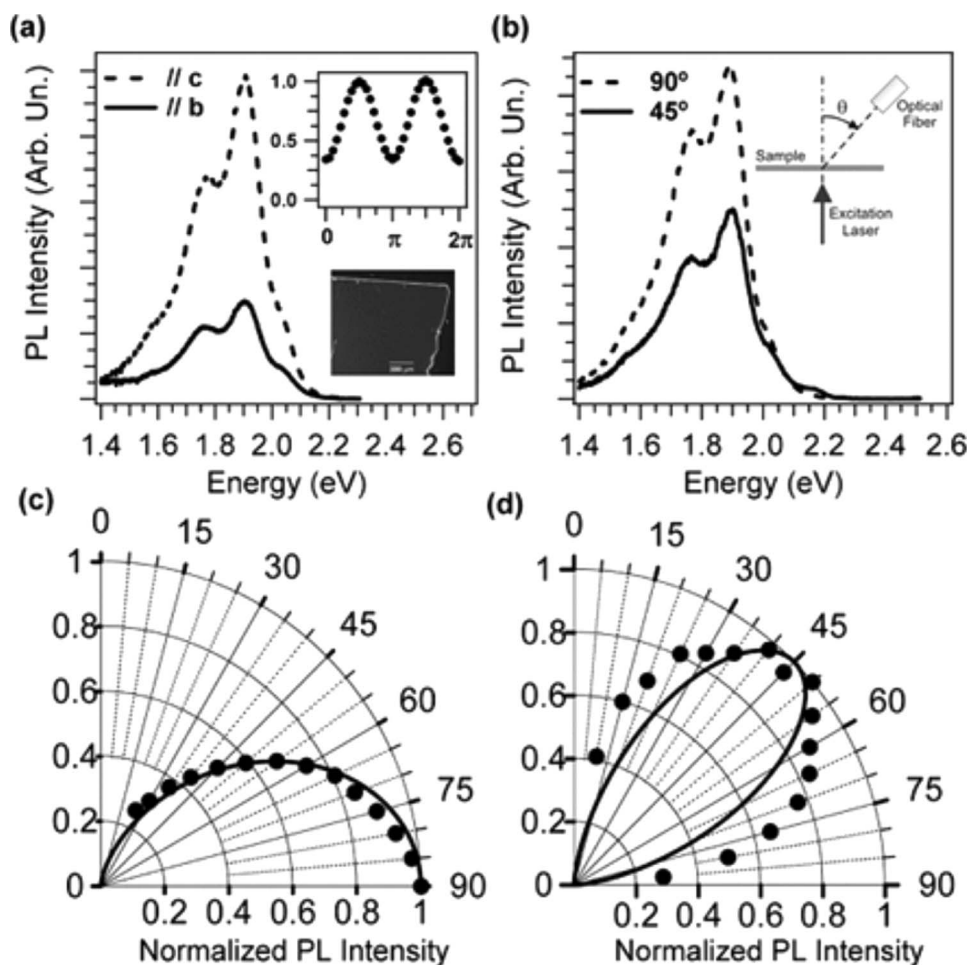


FIG. 3. (a) Polarized PL spectra acquired from the edge of the crystal along the direction of the a axis, with the analyzer along the b (continuous line) and the c axis (dashed line). Inset: normalized PL intensity as a function of the angle formed by the analyzer axis and the b axis. Inset: Image of a rubrene crystal as taken under the fluorescence microscope. (b) PL spectra acquired at a collection angle of 90° and 45° , the surface normal and the direction of collection lying in the ac plane of rubrene. Inset: Scheme of the setup used for angle-resolved PL measurements. (c,d) Angular distribution of the normalized PL intensity integrated over the whole energy range (c) or taken at 2.17 eV (d), together with the calculated distribution curves for a c polarized emitting dipole (c) and for a c polarized emitting dipole taking into consideration the reabsorption by the resonant c polarized absorption transition.

mean-squared error which changes from 2.47 (bulk) to 2.60 (bulk+EMA layer). For this reason, we believe that the presence of a surface-graded oxidized layer does not prevent the determination of reliable optical functions of the rubrene bulk.

In Fig. 3(a) we report the spectra of the emission propagating along the a direction with the analyzer along either c or b . The c polarized intensity is about 3 times larger than the b polarized one [inset of Fig. 3(a)]. Similar results are obtained analyzing the emission propagating in the b direction polarized in the ac plane. We conclude that the emission from the crystal edges is polarized along c . The presence of some a and b polarized emission from the crystal edge is attributed to the irregular shape of the crystal border. The inset of Fig. 3(a) shows an image of a rubrene crystal. It is evident that there is no relevant surface emission and that light is self-guided. This property was also evidenced by exciting only the central part of the sample by a laser beam (1 mm^2 spot size) and detecting the photoluminescence from the crystal edges, 1–2 mm away from the illuminated region. At the edge, c polarized light is emitted, together with some unpolarized intensity diffused from the border and clearly observed in the image in the inset of Fig. 3(a) taken from the top. A detailed analysis of light propagation confirms that the c polarized emitted radiation is confined inside the crystal and self-guided to the edges. Indeed, on the basis of the known dielectric tensor we found that the light propa-

gating inside the crystal at an angle to the surface-normal greater than a limit value of about 42° is totally reflected back into the sample for every polarization, every direction of propagation, and in the whole PL spectral region. For several directions of propagation, this limit angle is even lower, so that, considering the typical angular distribution from an emitting dipole,²⁴ almost the whole emission is totally reflected. We also calculated that emitted light can couple to the crystal guided modes in the whole PL spectral range.²⁵ The intensity angular dependence confirms these findings. Also for other molecular materials, self-waveguided emission is reported in the literature, such as in the case of octithiophene crystals,²⁶ needle-shaped crystals of sexiphenyl,²⁷ and thiophene/phenylene crystals,²⁸ In the case of quaterthiophene crystals, this has been formally explained on the basis of the known material dielectric tensor.²⁹

Figure 3(b) shows the PL spectra at a collection angle of 90° and 45° (0° corresponds to the emission in the normal direction to the crystal surface). The PL intensity integrated in the whole spectral range [Fig. 3(c)] increases from 20° to 90° , in agreement with the predicted distribution for a c polarized dipole²⁴ also indicated for comparison. At 45° , besides the same PL peaks observed at 90° , a weak band is observed at 2.17 eV, that results to be c polarized from polarization analysis. The corresponding angular dependence in Fig. 3(d) shows the trend predicted for a c polarized emitting dipole after reabsorption by a c polarized resonant transition.

Finally, we compare our findings with the recent results of Najafov *et al.*³⁰ and of Mitrofanov *et al.*¹⁶ In both papers, a PL band is reported at 2.17 eV, together with a stronger emission at lower energies. The former has been attributed to the intrinsic excitonic emission of rubrene crystals, the latter has been attributed to a possible self-trapped molecular exciton by Najafov *et al.*, as demonstrated by the difference in the excitation spectrum with respect to the other PL bands and by the overlap between the bands observed in the PL emission and excitation spectra. The recent study of Mitrofanov *et al.*¹⁶ allowed to attribute this localized emission to the oxidized component. Our results give further insight into its *c* polarization and the propagation properties. The PL spectral features of rubrene correspond to the optical transitions observed in the *c* component of the dielectric tensor and belong to a different series with respect to those observed in normal-incidence absorption spectra. However, both the *c* transition of *M* origin and the *a* and *b* transitions of *LN* origin contribute to the population of the emitting level, as deduced by the continuous-wave excitation spectrum monitored at 2 eV shown in Ref. 30, where the different mechanisms responsible for the population are also discussed.

IV. CONCLUSIONS

The UV-VIS dielectric tensor of rubrene crystals is provided for the first time. The results give both experimental evidence and formal analysis to show that (i) emission belongs to a series with different origin with respect to the transitions which are probed in normal-incidence optical measurements; (ii) weak intermolecular interactions are found for the lowest optical transitions, thus determining a weak exciton delocalization; (iii) the emission is self-guided towards the edge where *c* polarized light is detected with the corresponding intensity angular distribution. In particular, we underline that it is well established for organic slabs that the thickness of the film is an important condition for waveguiding assisting stimulated emission. In this work, we also evidence the importance of polarization to get an effective self-guiding. The full optical characterization and the understanding of the intrinsic photo-excitation mechanisms open new possibilities for applications of rubrene in light emitting devices.

-
- ¹V. C. Sundar, J. Zaumseil, V. Podzorov, E. Menard, R. L. Willett, T. Someya, M. E. Gershenson, and J. A. Rogers, *Science* **303**, 1644 (2004).
- ²V. Podzorov, E. Menard, A. Borissov, V. Kiryukhin, J. A. Rogers, and M. E. Gershenson, *Phys. Rev. Lett.* **93**, 086602 (2004).
- ³T. Oyamada, H. Uchiuzou, S. Akiyama, Y. Oku, N. Shimoji, K. Matsushige, H. Sasabe, and C. Adachi, *J. Appl. Phys.* **98**, 074506 (2005).
- ⁴D. A. de Silva Filho, E.-G. Kim, and J.-L. Brédas, *Adv. Mater. (Weinheim, Ger.)* **17**, 1072 (2005).
- ⁵E. Menard, A. Marchenko, V. Podzorov, M. E. Gershenson, D. Fichou, and J. A. Rogers, *Adv. Mater. (Weinheim, Ger.)* **18**, 1552 (2006).
- ⁶W. Xie, Y. Zhao, J. Hou, and S. Liu, *Jpn. J. Appl. Phys., Part 1* **42**, 1466 (2003).
- ⁷D. E. Henn, W. G. Williams, and D. J. Gibbons, *J. Appl. Crystallogr.* **4**, 256 (1971).
- ⁸I. Bulgarovskaya, V. Vozzhennikov, S. Aleksandrov, and V. Bel'sky, *Latv. PSR Zinat. Akad. Vestis, Fiz. Teh. Zinat. Ser.* **4**, 53 (1983).
- ⁹O. D. Jurchescu, A. Meetsma, and T. T. M. Palstr, *Acta Crystallogr., Sect. B: Struct. Sci.* **B62**, 330 (2006).
- ¹⁰A. S. Davydov, *Theory of Molecular Excitons* (Plenum, New York, 1971).
- ¹¹G. M. Badger and R. S. Pearce, *Spectrochim. Acta* **4**, 280 (1951).
- ¹²J. Chang, D. M. Hercules, and D. K. Roe, *Electrochim. Acta* **13**, 1197 (1968).
- ¹³M. Kaschke, N. P. Ernsting, and F. P. Schafer, *Opt. Commun.* **66**, 211 (1988).
- ¹⁴Y. Hamada, H. Kanno, T. Tsujioka, H. Takahashi, and T. Usuki, *Appl. Phys. Lett.* **75**, 1682 (1999).
- ¹⁵A. Otomo, S. Otomo, S. Yokoyama, and S. Mashiko, *Opt. Lett.* **27**, 891 (2002).
- ¹⁶O. Mitrofanov, D. V. Lang, C. Kloc, J. M. Wikberg, T. Siegrist, W. Y. So, M. A. Sergent, and A. P. Ramirez, *Phys. Rev. Lett.* **97**, 166601 (2006).
- ¹⁷F. Wooten, *Optical Properties of Solids* (Academic Press, New York, 1972).
- ¹⁸G. Weiser and S. Moller, *Phys. Rev. B* **65**, 045203 (2002).
- ¹⁹R. M. A. Azzam and N. M. Bashara, *Ellipsometry and Polarized Light* (North-Holland, Amsterdam, 1997).
- ²⁰M. Schubert, B. Rheinlander, E. Franke, H. Neumann, T. E. Tiwald, J. A. Woollam, J. Hahn, and F. Richter, *Phys. Rev. B* **56**, 13306 (1997).
- ²¹M. Born and E. Wolf, *Principles of Optics* (Pergamon Press, New York, 1965).
- ²²D. Käfer and G. Witte, *Phys. Chem. Chem. Phys.* **7**, 2850 (2005).
- ²³D. E. Aspnes, *Thin Solid Films* **89**, 249 (1982).
- ²⁴J. A. Stratton, *Electromagnetic Theory* (McGraw-Hill, New York, 1941).
- ²⁵F. Hide, M. A. Diaz-García, B. J. Schwartz, M. R. Andersson, Q. Pei, and A. J. Heeger, *Science* **273**, 1833 (1996).
- ²⁶D. Fichou, S. Delysse, and J. M. Nunzi, *Adv. Mater. (Weinheim, Ger.)* **9**, 1179 (1997).
- ²⁷H. Yanagi, T. Ohara, and T. Morikawa, *Adv. Mater. (Weinheim, Ger.)* **13**, 1452 (2001).
- ²⁸M. Ichikawa, R. Hibino, M. Inoue, T. Haritani, S. Hotta, T. Koyama, and Y. Taniguchi, *Adv. Mater. (Weinheim, Ger.)* **15**, 213 (2003).
- ²⁹S. Tavazzi, P. Spearman, L. Silvestri, L. Raimondo, A. Camposo, and D. Pisignano, *Org. Electron.* **7**, 561 (2007).
- ³⁰H. Najafov, I. Biaggio, V. Podzorov, M. F. Calhoun, and M. E. Gershenson, *Phys. Rev. Lett.* **96**, 056604 (2006).